


 Cite this: *RSC Adv.*, 2023, **13**, 22216

# Characteristics and health risk assessment of heavy metals in dust of a waste printed circuit board recycling workshop, China

 Ye Wang, <sup>ab</sup> Jingru Xu<sup>a</sup> and Guijian Liu<sup>\*a</sup>

Physical separation is the most widely used technology concerning waste printed circuit board (WPCB) recycling in practical terms. The dust generated from the process poses a significant environmental and human health risk. Amounts of heavy metals in dust present in each processing zone of the workshop showed differences. However, to date, few studies have reported this. The mean metal concentrations in workshop dust from different processing zones were investigated in this study and it was found that Zn, Pb, and Sn appeared in higher levels than other metals, followed by Mn > Cr > Ni > V > As > Cd. The enrichment factors (EFs) ranged from 1.15 to 207.4, and decreased in the order of Cu > Sn > Pb > Zn > Cd > Cr > Ni > V > As, which was exactly consistent with the geo-accumulation index values. The comparison of the EF values of workshop dust in and outside showed that the EFs in workshop dust were mostly smaller. Metals in the dust of the crushing zone (CrZ) showed significant and strong enrichment. The non-carcinogenic risk for different processing zones was all less than 1, which is recognized safety for people's health. The total carcinogenic risk from Cr, and Ni in all zones and As in the CrZ exposure was not negligible. The carcinogenic and non-carcinogenic risks in the CrZ were significantly higher than in the other zones. Masks to filter dust, a ventilation system, daily work hours reduction, and automation improvement was proposed for reducing workers' exposure to heavy metal.

 Received 12th May 2023  
 Accepted 17th June 2023

DOI: 10.1039/d3ra03164k

[rsc.li/rsc-advances](http://rsc.li/rsc-advances)

## 1. Introduction

With the development of the electronics industry and acceleration of product replacement, the amount of waste printed circuit boards (WPCBs) has increased in recent years.<sup>1–4</sup> The WPCBs contain more than 60 metal substances,<sup>5</sup> including precious metals such as Pt, Au, and Pd,<sup>6–8</sup> and account for 40% of total metal recovery value of waste electronic and electrical equipment (WEEE).<sup>9,10</sup> Therefore, they have become a significant resource that can be recycled due to the high economic benefits.<sup>11,12</sup> However, because of various harmful heavy metals and organic pollutants contained in WPCBs, when WPCBs are recycled or discarded in an unfriendly manner, a threat to the environment and human health can be posed.<sup>13</sup> Because of this, there has been widespread concern regarding WPCBs for some time. Physical separation, hydrometallurgy, pyrolysis, pyrometallurgy, bio-metallurgy and supercritical fluid oxidation and other methods have been tried by many researchers to recover and extract valuable metal materials from WPCBs,<sup>14–16</sup> and reduce their harmful environmental impacts.<sup>11,17</sup> However, physical separation is still the most widely used technology in practical application due to its

low construction and operation costs, uncomplicated process, and acceptable economic and environmental options.

Physical separation, based on different physical properties of the metallic and nonmetallic materials,<sup>18</sup> is also usually used as a pretreatment process for metals enrichment.<sup>19–22</sup> Impurity metal elements, which have copper as their main component, have widely been used for copper smelting instead of some raw materials, while organic components are removed by the high temperature of the copper smelting furnace.<sup>12</sup>

Depending on the different separation mediums, physical separation was divided into dry separation and hydraulic separation, the latter was officially banned in certain regions of China, due to the generation of a large amount of wastewater containing various hazardous contaminants. The physical separation processes applied for the pretreatment include dismantling and crushing. According to the previous studies, the metal and nonmetal have almost completely dissociated when WPCBs are crushed into particles less than 0.6 mm,<sup>23,24</sup> therefore, two-step or three-step crushing processes with a shredder, hammer breaker and hammer-mill are proposed to achieve the process.<sup>25</sup> However, due to over-crushing, large amounts of fine particles attached to heavy metals and organic pollutants are released to the recycling workshop.<sup>18</sup> Although a lot of measures have been taken to enhance the efficiency of dust capture, preventing dust from escaping in the workshop, dust pollution has always been the most significant problem of dry physical separation.

<sup>a</sup>CAS Key Laboratory of Crust-Mantle Materials and Environment, School of Earth and Space Sciences, University of Science and Technology of China, Hefei, Anhui 230026, China. E-mail: [lgj@ustc.edu.cn](mailto:lgj@ustc.edu.cn); Fax: +86-551-63621485; Tel: +86-551-63603714

<sup>b</sup>Solid Waste Management Center of Anhui Province, Hefei, Anhui 230061, China



According to published results, long incubation periods and hard to degrade heavy metals, adhered to small particles and entering the environment and body, will cause pollution of the ecological environment and health risks to workers.<sup>13,22,26–28</sup> In recent years, many studies put emphasis on the pollutants release in WPCBs recycling process, especially for the various heavy metal contaminations. WPCBs with electronic components were collected as materials from WEEE recycling enterprises in previous studies,<sup>29,30</sup> and mostly the whole workshop was taken as a research object. Wang proposed that complex heavy metals and even persistent organic pollutants exist in electronic components.<sup>31</sup> However, the printed circuit board (PCB) manufacturing process is the other significant contribution to WPCBs generation, and China is the world's largest producer of PCB, the output reached 699 million square meters in 2019.<sup>32</sup> Due to the complicated production process and materials with various heavy metals used, the emission of heavy metals in defectives and offcuts recycling is worthy to concern.

Except for a few WPCBs generated from electrical dismantling, samples in this study were selected from an enterprise that supported the PCB manufacturing area; thereby, most materials were unqualified products and offcut produced by PCB manufacturers with no electronic components, except for few WPCBs generated from electrical dismantling. Samples from different working zones were collected to explore the characteristics, also health risks of heavy metals in different processing zones, then suggestions for pollution prevention and workers' protection in different zones were proposed. The experiments were carried out to (1) understand the heavy metals distribution, concentration, morphology and composition of dust in the workshop; (2) analyze the characteristics of heavy metals enrichment in the dust of different processing zones and compare them to dust taken from outside the workshop to detect the migration of dust; (3) evaluate the health risks to workers by heavy metals exposure in the workshop dust and propose suggestions for workers engaged in different processing zones.

## 2. Materials and methods

### 2.1 Samples

In this study, we selected a WPCBs recycling enterprise maintaining that has been in stable operating condition for a long

time in eastern China (Fig. 1). It was located in an industrial area that was home to more than forty PCB manufacturing companies. The WPCBs were generated primarily from PCB manufactured. A physical separation process combining magnetic separation, pneumatic separation, and electrostatic separation was taken for metal and non-metal separation of WPCBs. Each process in the workshop was partitioned into relatively independent zones by steel plate. Samples were collected in December 2021, from different zones including the feeding zone (FdZ), dismantling zone (DmZ), crushing zone (CrZ), WPCBs storage zone (WsZ), and powder storage zone (PsZ) respectively, in and around the workshop (Table 1). The FdZ was a widely open area for WPCBs feeding and transporting to crushing by conveyor belt. The CrZ was a completely enclosed space with a ventilation system for collection and filter for particulates. WsZ and PsZ in the workshop were both sealed off around and unroofed, for WPCBs and separated resin powder storing respectively. The DmZ was a small, separated room within a rarely used hot-air heated detinning machine. To obtain the accumulated dust in a certain period of time, we collected dust from windowsills, walls and outdoor windowsills in different zones that without cleaning up for a long time. We brushed the dust carefully with a brush when collecting samples, then put the samples into a sealed, labeled bag. Meanwhile, we collected samples outside window sill of the workshop except for samples in the workshop. Because FdZ was a separated and closed room rarely used, and WsZ was separated by a low flap from PsZ, total suspended particulates were collected in FdZ, PsZ and CrZ of the recycling workshop for twenty-three hours per day for three consecutive days. The quartz filter membrane was selected for the atmospheric particulates sampler and the air flow rate was 100 L min<sup>-1</sup>. All samples were taken back to the lab and stored in a refrigerator below 4 °C.

### 2.2 Heavy metal concentration measurement

**2.2.1 Sample preparation.** A total of 0.2 grams of dust was accurately weighed and placed into a microwave digestion tube, paying attention to wall sticking. An acid system consisting of 9 mL of nitric acid (65%), 3 mL of hydrochloric acid (38%), 3 mL of hydrofluoric acid (40%), and 0.5 mL of hydrogen peroxide

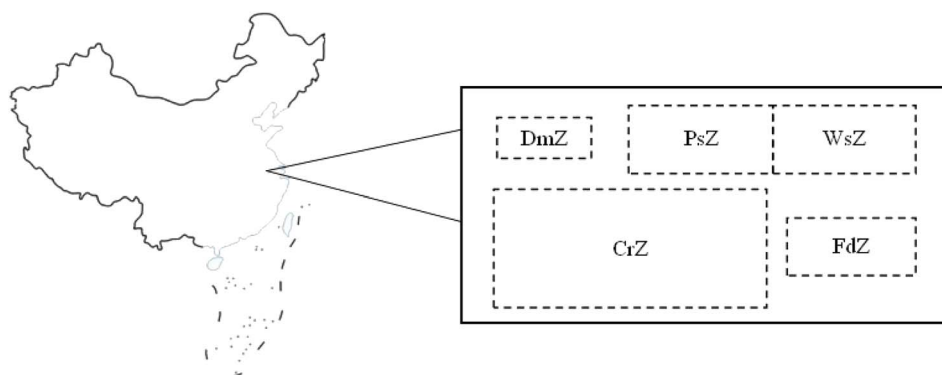


Fig. 1 Location and layout of sampling enterprise.



Table 1 Sampling details

	Area	Number	Time
Process area	FdZ	2	2021/12/17–2021/12/18
	DmZ	3	2021/12/17–2021/12/18
	CrZ	3	2021/12/17–2021/12/18
Storage area	WsZ	10	2021/12/17–2021/12/18
	PsZ	6	2021/12/17–2021/12/18

was used to digest the dust samples.<sup>13</sup> Then, the mixtures were heated to 185 °C by 3 heating progresses with a microwave digestion machine (Milestone ETHOS UP). According to the Chinese National Environmental Protection Standard HJ803-2016,<sup>33</sup> the inductively coupled plasma mass spectrometry (ICP-MS, PerkinElmer NexION 350D, US) was used to determine the concentrations of heavy metals in sample solutions after pretreatment.

**2.2.2 Quality control.** The experiments in this study were subjected to quality control. The experimental digestion tube vessels were cleaned with nitric acid (50%), and then washed 3 times with tap water and 3 times with ultrapure water before being dried. Analysis for reagent blanks and certified reference samples were taken for quality controlling in each run. The limits of detection (LODs) and quantification (LOQs) for ICP-MS are listed in the Table 2. The determining coefficients of calibration curves for the measurement system reached to higher than 0.99, indicating high linearity, precision, and accuracy. The recovery rates of the detecting heavy metals ranged from 82.3% to 112.8%.

### 2.3 Particle morphology characteristics

Scanning Electron Microscopy (SEM, ZEISS GeminiSEM500) was used to analyze the micro-morphological characteristics of dust. All the samples were sprinkled over double-sided carbon tape and were mounted on an SEM. The surface morphology results were printed as black-and-white images.

### 2.4 Mineral composition analysis

In this study, an X-ray diffractometer (XRD) was used to analyze the mineral composition of dust in the workshop, and the measured lattice plane spacing and diffraction intensity are

Table 2 The limit of detection (LODs) and quantification (LOQs) for ICP-MS

Elements	LODs (mg kg <sup>-1</sup> )	LOQs (mg kg <sup>-1</sup> )
Cd	0.017	0.068
Cu	0.156	0.624
Cr	0.850	3.400
Mn	0.140	0.560
Ni	0.255	1.020
Pb	0.644	2.576
Zn	0.670	0.268
V	0.176	0.704
As	0.125	0.500

compared with the diffraction data of the standard phase, to explore the phase composition and main sources in samples.<sup>34</sup> The scan angle  $2\theta$  measured by XRD analysis was between 10 and 80°. The test results were analyzed using the International Diffraction Data Center (ICDD) PDF-2 (2014) database and MDI Jade 6.0 software.

### 2.5 Enrichment factors

The enrichment factor (EF) is usually used to present the enrichment degree of heavy metals in dust, and distinguish and evaluate the main source.<sup>35,36</sup> The values are calculated with the eqn (1) below:<sup>26,37,38</sup>

$$EF = \left( \frac{C_n}{C_{ref}} \right)_{\text{sample}} / \left( \frac{B_n}{B_{ref}} \right)_{\text{background}} \quad (1)$$

Where  $C_n$  is the concentration of the element and  $C_{ref}$  is the concentration of the reference element in the sample,  $B_n$  is the background value of the element and  $B_{ref}$  is the background value of the reference element. In this study, we selected Mn as the reference element.<sup>26</sup> Background values of elements in Chinese soils were used due to a lack of dust background value investigation.<sup>39–41</sup>

### 2.6 Geo-accumulation index

Except for the EFs, the geo-accumulation index ( $I_{geo}$ ) is also an indicator that can express the characteristics of heavy metals enrichment in the dust,<sup>42</sup> simultaneously, can indicate the impact on the environment caused by anthropogenic activity (Table 3).<sup>43</sup> The values are calculated by following eqn (2):

$$I_{geo} = \lg_2[C_{\text{sample}} / (1.5 \times C_{\text{background}})] \quad (2)$$

where  $C_{\text{sample}}$  is the concentration of the element and  $C_{\text{background}}$  is the background value of the element.

### 2.7 Health risk assessment

Workers working in workshops are exposed to dust generated from the recycling process, mainly in three ways of ingestion, inhalation and dermal contact.<sup>28,40,42–45</sup> Workers in different processing zones will be subjected to varying degrees of harm due to their different exposure to dust. In this study, based on the assumption that the particle size distribution of dust in workshops is similar to soil particle size distribution, the risk

Table 3 Geo-accumulation classes and their pollution status for dust quality

$I_{geo}$ value	$I_{geo}$ class	Qualitative designation
$\leq 0$	0	No contaminated
0–1	1	Slightly contaminated
1–2	2	Moderately contaminated
2–3	3	Moderately to heavily contaminated
3–4	4	Heavily contaminated
4–5	5	Heavily to extremely contaminated
$> 5$	6	Extremely contaminated



Table 4 Factors, definitions and values in eqn (3)–(5)

Factor (unit)	Definition	Values	Reference
ADD	Average daily exposure dose		
$C$ ( $\text{mg kg}^{-1}$ )	The concentration of heavy metals		This article
$\text{IngR}$ ( $\text{mg day}^{-1}$ )	Ingestion rate	30	46
$\text{InhR}$ ( $\text{m}^3 \text{day}^{-1}$ )	Inhalation rate	20	47
$\text{PEF}$ ( $\text{m}^3 \text{kg}^{-1}$ )	Particle emission factor	$1.36 \times 10^9$	48
$\text{SL}$ ( $\text{mg cm}^{-2}$ per day)	Skin adherence factor	0.07	48
$\text{SA}$ ( $\text{cm}^2$ )	Exposed skin area	5700	49
ABS	Dermal absorption factor	Cd: 0.001; Ni, Pb: 0.1; As: 0.03	50
EF (days per year)	Exposure frequency	262.5	51
ED (years)	Exposure duration	24	49
BW (kg)	Body weight	56.8	51
AT	Averaging time	Non-cancer: $\text{ED} \times 365$ Cancer: $70 \times 365$	49 51

assessment method was adopted.<sup>26,41</sup> The average daily exposure dose (ADD) through three pathways was calculated by eqn (3)–(5) respectively. Table 4 displays the values and parameters used to calculate the ADDs.

$$\text{ADD}_{\text{ing}} = C \times \frac{\text{IngR} \times \text{EF} \times \text{ED}}{\text{BW} \times \text{AT}} \times 10^{-6} \quad (3)$$

$$\text{ADD}_{\text{inh}} = C \times \frac{\text{InhR} \times \text{EF} \times \text{ED}}{\text{PEF} \times \text{BW} \times \text{AT}} \quad (4)$$

$$\text{ADD}_{\text{der}} = C \times \frac{\text{SL} \times \text{SA} \times \text{ABS} \times \text{EF} \times \text{ED}}{\text{BW} \times \text{AT}} \times 10^{-6} \quad (5)$$

Because dust in the air settlements in workers' respiratory through breathing, the concentrations of heavy metals in suspended particulates in the air were taken for calculating the  $\text{ADD}_{\text{inh}}$ .

The hazard quotient (HQ), indicating the non-carcinogenic impact of an element of heavy metal in workshop dust, was calculated with eqn (6). The hazard index (HI), the sum of HQs, represents the risk through the mentioned three ways.<sup>47</sup> If the  $\text{HQ} < 1$ , it shows that non-carcinogenic risks are insignificant. If the  $\text{HQ} \geq 1$ , the non-carcinogenic effects are possible. The carcinogenic risk (CR) is usually used to evaluate carcinogenic hazards of exposure in someone's lifetime. The total carcinogenic risk (TR), the sum of the CRs, represents the carcinogenic impact on workers for the three pathways. If the  $\text{CR}/\text{TR} < 1 \times 10^{-6}$ , shows carcinogenic risks are inappreciable. If the  $\text{CR}/\text{TR}$  is in the range of  $1 \times 10^{-6}$  to  $1 \times 10^{-4}$ , adverse carcinogenic risks are acceptable or tolerable, and  $\text{CR}/\text{TR} > 1 \times 10^{-4}$  indicates that cancer may appear 1 in 10 000 people for their exposure to carcinogenic risks in a lifetime.<sup>26,52,53</sup>

The following eqn (6)–(9) showed the calculation methods:<sup>54–56</sup>

$$\text{HQ} = \frac{\text{ADD}_{\text{ing/inh/der}}}{\text{RfD}} \quad (6)$$

$$\text{HI} = \sum \text{HQ} \quad (7)$$

$$\text{CR} = \text{ADD}_{\text{ing/inh/der}} \times \text{SF} \quad (8)$$

$$\text{TR} = \sum \text{CR} \quad (9)$$

where, RfD and SF represent respectively the homologous reference dose and the homologous slope factor.<sup>35,42,50,57–60</sup>

## 3. Results and discussion

### 3.1 Heavy metal concentration

The concentrations ( $\text{mg kg}^{-1}$ ) of heavy metals (Pb, Cr, As, Cd, Sn, Zn, V, Mn, and Ni) in the dust of different zones in the workshop are shown in Table 5. The mean concentration values in dust decreased in the order of  $\text{Zn} > \text{Pb} > \text{Sn} > \text{Mn} > \text{Cr} > \text{Ni} > \text{V} > \text{As} > \text{Cd}$ . Pb, Sn, and Ni, are representative heavy metals in WPCB,<sup>13</sup> released into the workshop attached to small particles,<sup>60</sup> then partly larger particles accumulated in the dust by their gravity and external disturbance.

The concentrations of heavy metals in storage areas including WsZ and PsZ were both in this order except for  $\text{Mn} > \text{Sn}$  in WsZ, which was less exposed to crushing and separation because of a sealed-off around structure. Hence, explanation for the concentrations of heavy metals might be the natural particles on WPCBs. But we found the concentrations of heavy metals in processing zones including FdZ, DmZ and CrZ, were all ranked in the order of  $\text{Pb} > \text{Zn} > \text{Mn} > \text{Sn}$ , except for  $\text{Sn} > \text{Mn}$  in CrZ. Comparing concentrations of typical harmful heavy metals including Pb, Cr, As and Cd in dust, showed that Pb was the largest proportion in different zones in the workshop except for the CrZ for Cr. In general, the result was consistent with Wang's<sup>30</sup> report. However, the heavy metals especially for Pb were significantly lower than in a closed dismantling workshop for WPCBs with components,<sup>13</sup> demonstrating that the environmental influences of defective PCB recycling process were relatively lower.

### 3.2 Morphology

The morphological analysis of dust using the SEM was shown in Fig. 2. There were a variety of particle morphologies, such as rod-like particles, irregular particles, platy particles, the aggregates of rod-like particles, the aggregates of columnar particles and irregular particles, *etc.* The rod-like and rod-like aggregates



Table 5 Concentrations of heavy metals in dust of different zones in the workshop

Zone		Pb	Cr	As	Cd	Sn	Zn	V	Mn	Ni
FdZ	Average	300.90	94.71	1.51	0.17	142.39	190.44	19.79	191.70	65.27
	SD	64.03	25.24	0.00	0.05	28.15	59.54	4.52	103.08	48.77
DmZ	Average	211.12	66.28	ND	0.30	95.09	181.75	19.69	119.67	10.74
	SD	60.87	4.40	—	0.05	17.56	31.13	0.24	19.35	2.30
CrZ	Average	152.92	44.16	29.14	0.18	556.23	100.87	16.92	61.48	35.85
	SD	43.07	5.86	0.62	0.04	85.51	28.01	2.19	15.61	19.08
WsZ	Average	192.98	64.98	3.46	0.16	106.27	271.49	20.99	149.86	25.10
	SD	77.40	12.16	1.90	0.02	36.08	193.21	0.60	48.40	16.60
PsZ	Average	190.22	69.16	1.09	0.17	83.12	222.91	22.36	99.05	18.78
	SD	103.51	16.91	1.02	0.01	58.53	127.53	0.63	6.29	10.71
Max		373.92	112.56	29.78	0.35	638.49	627.44	22.98	264.59	99.76
Min		90.01	39.67	0.32	0.12	34.04	83.50	16.40	61.48	9.93
Total	Average	198.54	66.06	7.56	0.18	158.34	220.05	20.56	125.82	26.42
	SD	81.05	17.01	10.84	0.05	160.62	147.39	2.08	52.93	21.43
Background values		26.0	61.0	11.2	0.097	2.60	74.2	82.4	583	26.9

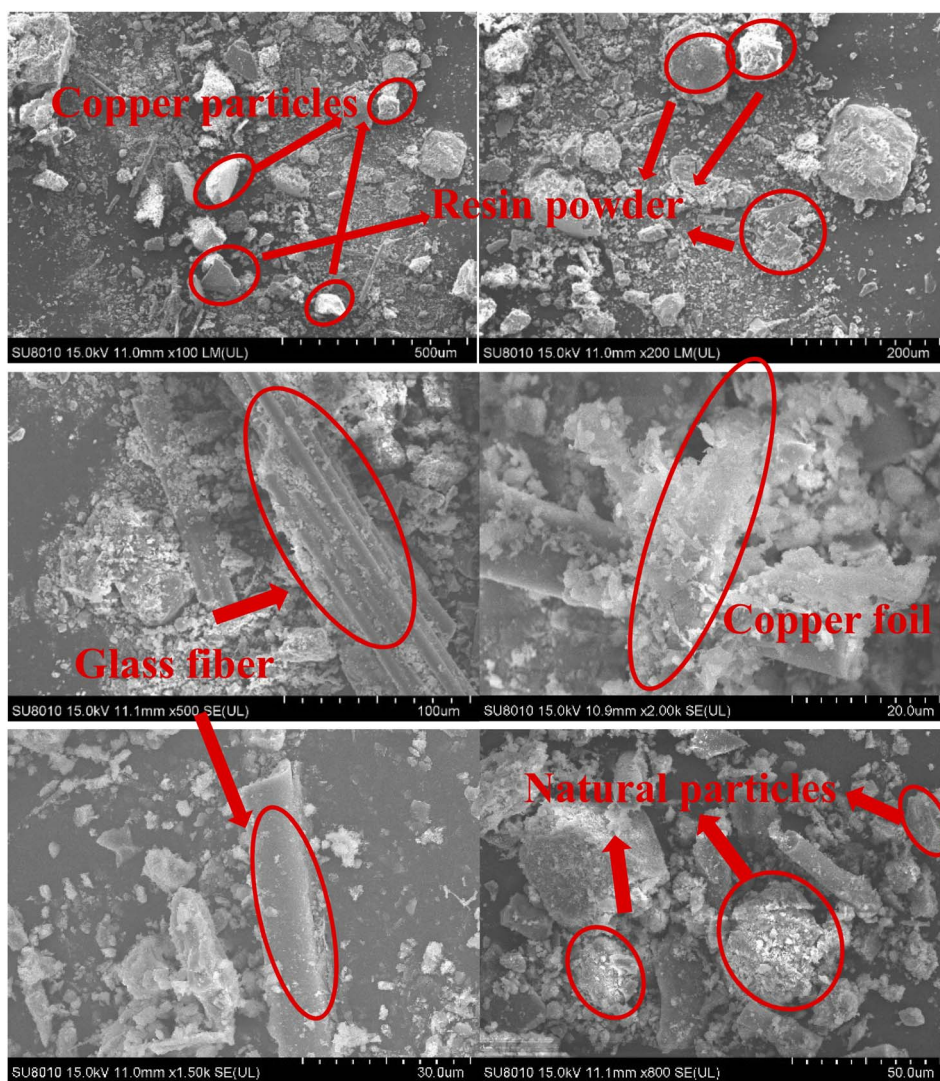


Fig. 2 SEM image of dust in the workshop.



particles were glass fibers added to PCBs for strength increase.<sup>16,61</sup> Because of the brittleness of WPCBs substrate materials, resin particles presented sharp-edge characteristics, which were different from the slightly curly features of copper with good toughness. The irregular particles adhered to particulates demonstrated natural particles.<sup>13,41</sup> The wide particle size distribution in workshop dust was shown, ranging from hundreds of microns to  $<1\ \mu\text{m}$ . Then, it could be found that some smaller particles attached to the larger particles.

### 3.3 Mineral composition

The mineral composite of dust was analyzed using XRD, the results were shown in Fig. 3. Dust particles in the workshop were mainly composed of Cu, Cr and other metal elements, which existed in the metallic state. It could be seen obviously that there were many amorphous peaks in the XRD pattern due to the poor crystallinity of organic substances in the dust.<sup>62</sup> While, the dust outside of the workshop was mainly composed of quartz, bismuth oxide and moganite, which mainly derived from the natural source.<sup>63</sup> So, it represented that the impact on surroundings caused by dust generated from WPCBs recycling had been limited.

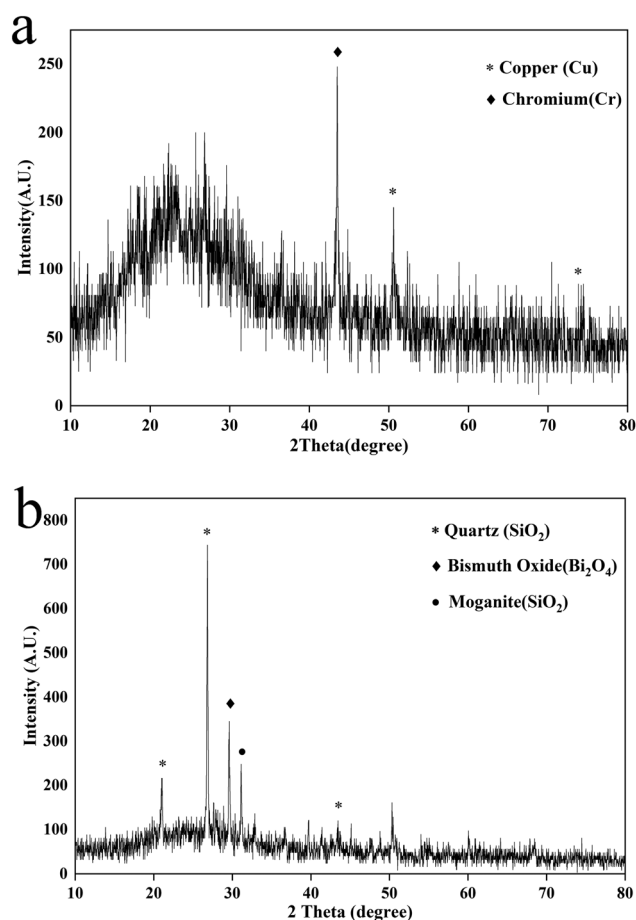


Fig. 3 XRD pattern of dust. (a) Dust in the workshop. (b) Dust outside of the workshop.

### 3.4 Enrichment characteristics of heavy metals

**3.4.1 Enrichment factors.** According to eqn (1), the EF values of heavy metals in the dust of workshop were calculated (Fig. 4). The median EFs of heavy metals were decreased in the order of  $\text{Cu} > \text{Sn} > \text{Pb} > \text{Zn} > \text{Cd} > \text{Cr} > \text{Ni} > \text{V} > \text{As}$  (Fig. 4a). It was obvious that the EF values of Cu (207.4) and Sn (173.57) were much higher than 100. That was seen in all processing zones, demonstrating strong enrichment. The EFs of Pb (34.22) and Zn (12.62) were both between 10 and 100, suggesting moderate enrichment. Furthermore, the EFs of Cd (9.25), Cr (5.53), Ni (3.44), V (1.38) and As (1.15) were all between 1 and 10, suggesting there was minimal influence of human activity on enrichment in dust of these heavy metals, and natural sources were main originators. The EF values of V (1.38) and As (1.15) were close to 1, indicating that these were obtained from a natural source.<sup>38</sup> The EFs of Pb were the highest of the values of typical hazardous heavy metals including Pb, As, Cr, and Cd.

A comparison of EFs of heavy metals in dust in and outside the workshop was shown in Fig. 4b. Except for V (0.74), the EF values of heavy metals in the dust on windowsills outside the workshop were all greater than one, showing that these heavy metals were enriched to varying degrees in outside workshop dust. Some of outside workshop dust were from artificial sources, mainly escaping dust with small particle sizes from the physical crushing and separation process in the workshop. However, compared with those of dust in the workshop, the EFs of these elements in outside workshop dust were larger except for Cu (51.84), Cr (5.15) and V (0.74), showing heavy metals tend to enrich in the dust with small particle size, which was consistent with previous reports that particles with smaller size had larger specific surface area and metal-adsorption capacity.<sup>13,18</sup> The EF value of Cu in outside workshop window sill dust is much lower than it is in workshop dust, indicating Cu was much more abundant in the dust with bigger particles due to its toughness.<sup>18</sup>

Comparing the EF values of dust in different processing zones (Fig. 4c) showed that the EFs of all heavy metals in the CrZ was the largest. The EFs of these heavy metals in the CrZ were higher than 10 except for Cr (6.46) and V (1.82), demonstrating moderate to strong enrichment. The EFs of Cr (6.46) and V (1.82) in CrZ are minimally enriched. Meanwhile, it showed that the EF of As (23.34) in CrZ was significantly higher than the values in other process zones, indicating enrichment in workshop dust of As originated mainly from the crushing process. Moreover, a study of the EFs of dust in various storage sites, including WsZ and PsZ, revealed that all heavy metals were more abundant in the PsZ.

**3.4.2 Geoaccumulation index.** The  $I_{\text{geo}}$  value of heavy metals in dust was calculated by eqn (2) (Fig. 5). The median  $I_{\text{geo}}$  values of Cu (4.86) and Sn (4.76) were significantly higher than other metals in dust, following the order of  $\text{Pb} (2.18) > \text{Zn} (0.56) > \text{Cd} (0.23)$ , showed slight to heavy-extreme enrichment. The median  $I_{\text{geo}}$  values of Cu and Sn were between 4 and 5, and the  $I_{\text{geo}}$  classes were 5, demonstrating heavy to extreme enrichment. The median  $I_{\text{geo}}$  values of Cr, As, V and

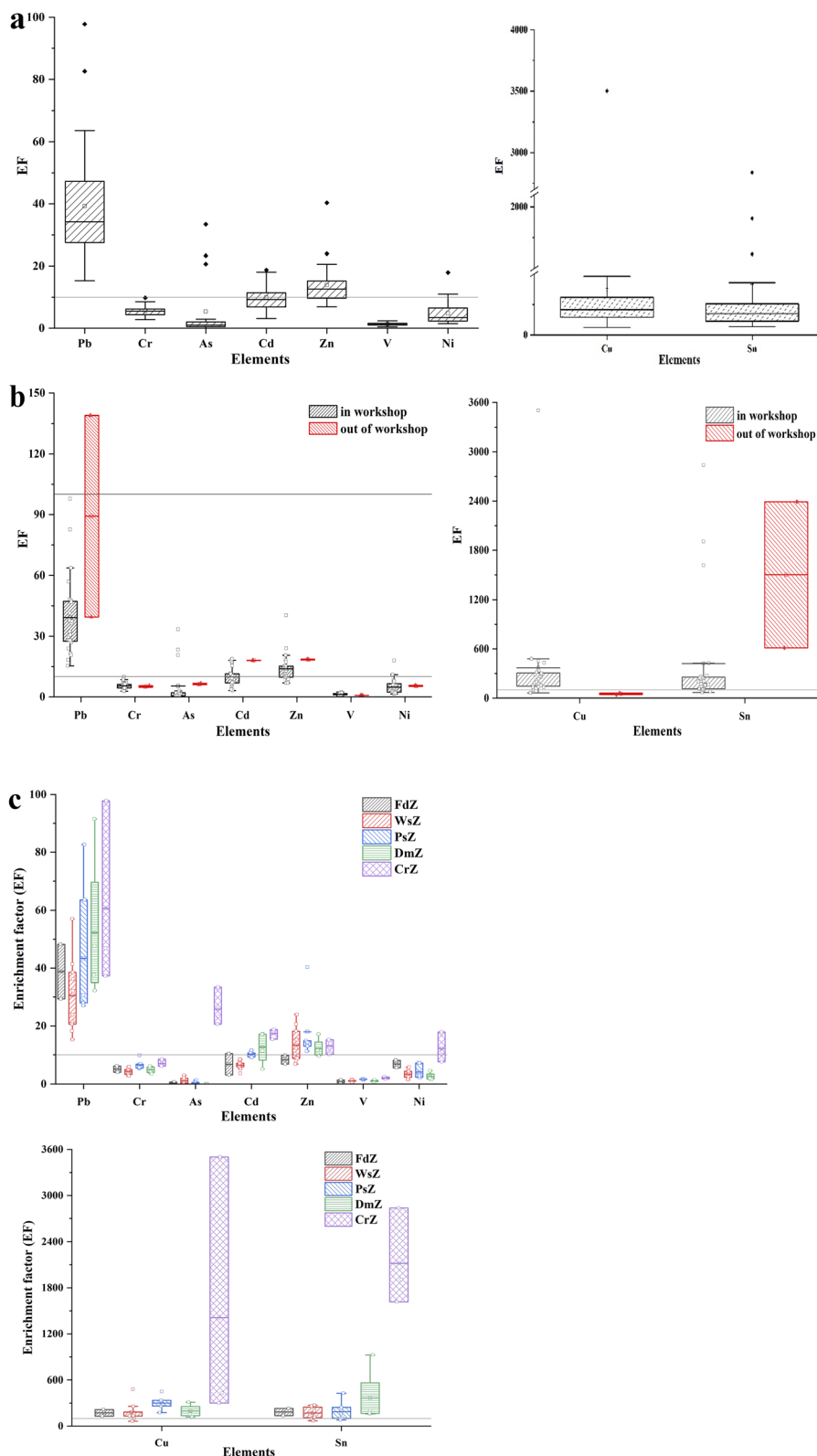


Fig. 4 EFs of heavy metals in dust in the workshop of different zones and dust outside the workshop. (a) EFs of heavy metals in dust in the workshop. (b) EFs of heavy metals in and out of the workshop. (c) EFs of heavy metals in different zones of the workshop.

Ni were lower than 0, and their  $I_{geo}$  class was 0, showing no enrichment and contamination, which was the same as the EFs results.

When the  $I_{geo}$  values of heavy metal in and outside the workshop dust were compared (Fig. 5b), it was obvious that the  $I_{geo}$  values in outside workshop dust were obviously higher than



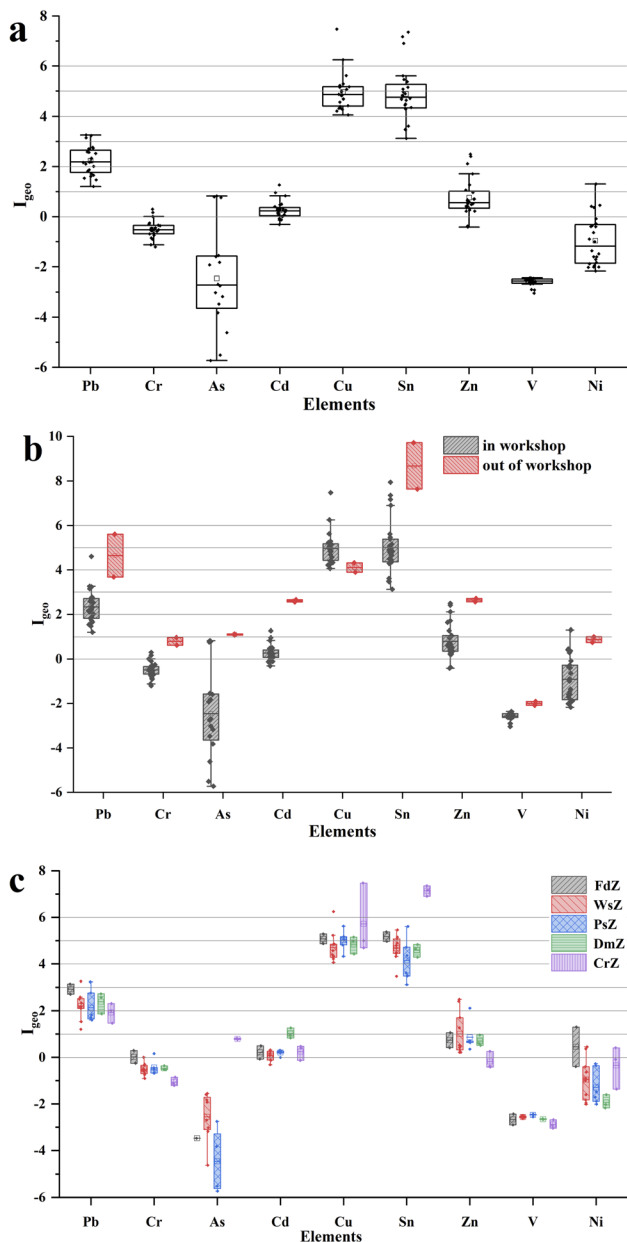


Fig. 5  $I_{geo}$  of heavy metals in dust in the workshop and outside the workshop in different processing zones. (a)  $I_{geo}$  of heavy metals in dust in the workshop. (b)  $I_{geo}$  in dust in workshop and outside the workshop. (c)  $I_{geo}$  in different processing zones.

those in the workshop dust except for Cu, which was consistent with the EFs. The  $I_{geo}$  class of Sn in and outside the workshop dust were both 6, while the  $I_{geo}$  value outside the workshop was much higher. The  $I_{geo}$  class of Pb in outside the workshop dust was 5, while that in the workshop dust was 3. So, it could be seen that Sn and Pb originated from releasing dust and tended to enrich in dust with small particle sizes, which represented a similar result to the EF. The results were in accordance with previous studies. The  $I_{geo}$  value of Cr, As and Ni in workshop dust were all lower than 0, but in outside dust, the  $I_{geo}$  values were significantly increasing and higher than 0, which representing enrichment.

Comparing with the  $I_{geo}$  values of dust in different processing zones (Fig. 5c), we found that the  $I_{geo}$  values of Sn, Cu, and As in the CrZ were significantly higher than other processing zones, which was in keeping with the EF results roughly. The  $I_{geo}$  class in the CrZ of Sn and Cu were 6, indicating extremely contaminated. Therefore, it could be seen that Sn and Cu in workshop dust mainly originated from WPCBs crushing and separating process. It reminded us that cleaned dust in the workshop, especially in CrZ, should be properly collected and disposed of to prevent environmental risk. It showed that the  $I_{geo}$  value of As in the CrZ was close to 1, much higher than that in other processing zones, demonstrating slightly contaminated. The  $I_{geo}$  values of Cu, Sn and Pb in all processing zones were all higher than 0, and the  $I_{geo}$  values of Cr and V in different processing zones in the workshop were both less than 0, this result was the same as the EF result. However, the  $I_{geo}$  values of Cd in each processing zone in the workshop were between 0 and 1, showing slight enrichment, which was not exactly consistent with the EF result. The reasons for the different final results might have been because the two calculation methods had a different emphasis, the environmental sensitivity of heavy metal was considered in  $I_{geo}$  and each processing zone was similar with slight differences. It could be found that Cr, Ni and V indicated indistinctive enrichment characteristics, which was same to the EF result.

### 3.5 Health risk assessment

In this study, the health risk caused by heavy metals on workers exposed to workshop dust in different processing zones of WPCBs physical separation was evaluated by using eqn (3)–(9). The HIs and TRs calculated for workers in different processing zones through three pathways mentioned above were presented in Table 6. The HIs were ranked in the order of Cu > Pb > As > Cr > Mn > Ni > V > Zn > Sn > Cd for workers in the workshop. It obviously showed the HQs of Cu were the highest in all zones, which contributed 67.4%, 75.9% and 80.0% to HI in FdZ, PsZ and CrZ respectively. When the non-carcinogenic risk of various processing zones in the workshop was compared, the HIs of CrZ were higher than other zones in the workshop. For all this, all HIs were lower than 1, which was internationally recognized as safety. However, the findings of the study that compared the HIs of the various processing zones demonstrated that workers in the CrZ were subjected to higher health risks. Hence, protection for workers in the workplace needs to be a primary priority.

The TRs for carcinogenic effects were ranked in the order of Ni > Cr > Pb > As > Cd in the FdZ, Cr > Ni > As > Pb > Cd in the PsZ, and Ni > As > Cr > Pb > Cd in the CrZ. Although the orders of risk in the various processing zones were somewhat varied, they clearly showed the highest CRs of Ni and Cr in all zones. The CR values for Ni and Cr, which were both higher than  $10^{-6}$ , expressed that the carcinogenic risk caused by exposure to Cr and Ni was considerable. This result was consistent with the conclusion of Zhou.<sup>13</sup> Compared to TRs in different zones of the workshop, the values in the FdZ and CrZ were relatively higher than the storage zone, indicating that there was a health risk associated with long-term exposure to



Table 6 HIs and TRs of metals in workshop dust in different processing zones

Metal	Pb	Cr	As	Cd	Ni	Cu	Sn	Zn	V	Mn	Sum
FdZ HI	$3.28 \times 10^{-2}$	$1.20 \times 10^{-2}$	$1.93 \times 10^{-3}$	$6.59 \times 10^{-5}$	$2.35 \times 10^{-3}$	$1.10 \times 10^{-1}$	$9.03 \times 10^{-5}$	$2.41 \times 10^{-4}$	$8.36 \times 10^{-4}$	$3.04 \times 10^{-3}$	$1.63 \times 10^{-1}$
TR	$3.36 \times 10^{-7}$	$6.17 \times 10^{-6}$	$2.99 \times 10^{-7}$	$3.47 \times 10^{-9}$	$1.61 \times 10^{-5}$						$2.29 \times 10^{-5}$
PsZ HI	$2.07 \times 10^{-2}$	$8.76 \times 10^{-3}$	$1.40 \times 10^{-3}$	$6.51 \times 10^{-5}$	$7.59 \times 10^{-4}$	$1.09 \times 10^{-1}$	$5.29 \times 10^{-5}$	$2.82 \times 10^{-4}$	$9.45 \times 10^{-4}$	$1.57 \times 10^{-3}$	$1.44 \times 10^{-1}$
TR	$2.13 \times 10^{-7}$	$4.51 \times 10^{-6}$	$2.19 \times 10^{-7}$	$7.37 \times 10^{-9}$	$6.19 \times 10^{-6}$						$1.11 \times 10^{-5}$
CrZ HI	$1.67 \times 10^{-2}$	$5.59 \times 10^{-3}$	$3.70 \times 10^{-2}$	$6.74 \times 10^{-5}$	$1.60 \times 10^{-3}$	$2.53 \times 10^{-1}$	$3.52 \times 10^{-4}$	$1.28 \times 10^{-4}$	$7.15 \times 10^{-4}$	$9.74 \times 10^{-4}$	$3.16 \times 10^{-1}$
TR	$1.73 \times 10^{-7}$	$2.88 \times 10^{-6}$	$5.70 \times 10^{-6}$	$3.46 \times 10^{-9}$	$1.47 \times 10^{-5}$						$2.35 \times 10^{-5}$

FdZ and CrZ. To reduce workers' exposure to heavy metals, a mask with filter dust and a ventilation system should be combined,<sup>28</sup> and daily work hours reduction could be a concern. Meanwhile, less manual operation and more mechanized replacement are trends for development, which are significant for promotion of the efficiency and occupational health and protection.

## 4. Conclusions

The study investigated the concentrations of Pb, Cr, As, Cd, Cu, Sn, Zn, V, Ni, and Mn in workshop dust resulting from the physical separation of WPCBs. The average metal concentrations in workshop dust were ranked in the order of Zn > Pb > Sn > Mn > Cr > Ni > V > As > Cd. The EFs of heavy metals were decreased in the order of Cu > Sn > Pb > Zn > Cd > Cr > Ni > V > As, while the  $I_{geo}$  values of heavy metals were ranked in different order. The EF values of these elements in outside workshop dust were higher than the values in workshop dust, which was consistent with the performance of  $I_{geo}$  values, indicating that heavy metals released during the crushing and separation of WPCBs were enriched in the dust with smaller particle sizes. The EF values in CrZ were significantly higher than the values in other processing zones. The metals in the dust of the crushing zone showed significant and strong enrichment compared with other processing zones. In the meanwhile, the  $I_{geo}$  values exhibited a general consistency. The HIs of different processing zones were in the following: FdZ > PsZ > CrZ. Generally, all HIs were lower than 1, which was a widely accepted safe range. In the workshop range, the TRs were ranked in the order of Ni > Cr > As > Pb > Cd, with minor variations in various processing zones. The CRs from Cr, and Ni in all zones as well as in the CrZ exposure were not negligible. The HIs and TRs in different processing zones were slightly different, however, exposure to higher health risks in CrZ was the same. The risk of heavy metals exposure through ingestion was higher than the other two pathways. Therefore, protection for workers in the workshop by means of reducing exposure through ingestion, inhalation and dermal contact should be addressed seriously, especially for those who work in the crushing and separation zone.

## Conflicts of interest

There are no conflicts of declare.

## Acknowledgements

The work was supported by the National Key R&D Program of China (2020YFC1908601).

## References

- S. Schwarzer, A. De Bono, G. Giuliani, S. Kluser and P. Peduzzi, *Environment Alert Bulletin*, 2005, vol. 5.
- J. Guan, J. W. Wang, X. Min and W. J. Wu, *Procedia Environ. Sci.*, 2012, **16**, 461–468.
- X. L. Zeng, L. X. Zheng, H. H. Xie, B. Lu, K. Xia, K. M. Chao, W. D. Li, J. X. Yang, S. Y. Lin and J. H. Li, *Procedia Environ. Sci.*, 2012, **16**, 590–597.
- P. Hadi, M. Xu, C. S. Lin, C.-W. Hui and G. McKay, *J. Hazard. Mater.*, 2015, **283**, 234–243.
- J. S. Yang, H. F. Wang, G. W. Zhang, X. J. Bai, X. L. Zhao and Y. Q. He, *Resour. Conserv. Recycl.*, 2019, **146**, 264–269.
- A. Puca, M. Carrano, G. Liu, D. Musella, M. Ripa, S. Viglia and S. Ulgiati, *Resour. Conserv. Recycl.*, 2017, **116**, 124–136.
- S. Holgersson, B. M. Steenari, M. Björkman and K. Cullbrand, *Resour. Conserv. Recycl.*, 2018, **133**, 300–308.
- T. Y. Huang, J. Zhu, X. F. Huang, J. J. Ruan and Z. M. Xu, *Waste Manage.*, 2022, **139**, 105–115.
- L. H. Yamane, V. T. de Moraes, D. C. R. Espinosa and J. A. S. Tenório, *Waste Manage.*, 2011, **31**, 2553–2558.
- A. Golev and G. D. Corder, *Miner. Eng.*, 2017, **107**, 81–87.
- J. F. He and C. L. Duan, *Waste Manage.*, 2017, **60**, 618–628.
- X. B. Wan, P. Taskinen, J. J. Shi, L. Klemettinen and A. Jokilaakso, *Miner. Eng.*, 2021, **160**, 106709.
- X. Y. Zhou, Master thesis, East China University of Science and Technology, 2014.
- A. Akcil, C. Erust, C. S. Gahan, M. Ozgun, M. Sahin and A. Tuncuk, *Waste Manage.*, 2015, **45**, 258–271.
- M. Kaya, *Waste Manage.*, 2016, **57**, 64–90.
- C. C. Nie, Y. Y. Wang, H. Zhang, Y. K. Zhang, Y. Q. Zhang, Z. Q. Yan, B. Li, X. J. Lyu, Y. J. Tao and J. Qiu, *J. Clean. Prod.*, 2020, **258**, 120976.
- P. Feng, Z. Wang, L. Meng and Z. C. Guo, *Chem. Eng. Process.: Process Intensif.*, 2022, **173**, 108813.
- R. Wang, Master thesis, Shanghai Jiao Tong University, 2020.
- R. Estrada-Ruiz, R. Flores-Campos, H. Gámez-Altamirano and E. Velarde-Sánchez, *J. Hazard. Mater.*, 2016, **311**, 91–99.
- L. Meng, Z. Wang, Y. Zhong, L. Guo, J. Gao, K. Chen, H. Cheng and Z. Guo, *Chem. Eng. J.*, 2017, **326**, 540–550.



- 21 M. Arshadi, S. Yaghmaei and S. M. Mousavi, *Resour. Conserv. Recycl.*, 2018, **139**, 298–306.
- 22 E. R. Rene, M. Sethurajan, V. K. Ponnusamy, G. Kumar, T. N. B. Dung, K. Brindhadevi and A. Pugazhendhi, *J. Hazard. Mater.*, 2021, **416**, 125664.
- 23 C. Guo, H. Wang, W. Liang, J. G. Fu and X. Yi, *Waste Manage.*, 2011, **31**, 2161–2166.
- 24 Y. W. Yang, F. W. Sun and Z. X. Tie, *Appl. Mech. Mater.*, 2014, **666**, 383–387.
- 25 Q. Wang, B. G. Zhang, S. Q. Yu, J. J. Xiong, Z. T. Yao, B. A. Hu and J. H. Yan, *ACS Omega*, 2020, **5**, 17850–17856.
- 26 Z. Cheng, L. J. Chen, H. H. Li, J. Q. Lin, Z. B. Yang, Y. X. Yang, X. X. Xu, J. R. Xian, J. R. Shao and X. M. Zhu, *Sci. Total Environ.*, 2018, **619**, 621–629.
- 27 P. Xiong, X. T. Yan, Q. Q. Zhu, G. B. Qu, J. B. Shi, C. Y. Liao and G. B. Jiang, *Environ. Sci. Technol.*, 2019, **53**, 13551–13569.
- 28 A. Jafari, S. Asadyari, Z. Moutab Sahihazar and M. Hajaghadzadeh, *Environ. Geochem. Health*, 2023, 1–19.
- 29 A. O. Leung, N. S. Duzgoren-Aydin, K. Cheung and M. H. Wong, *Environ. Sci. Technol.*, 2008, **42**, 2674–2680.
- 30 J. Y. Wang, H. Chen, W. Y. Xia, L. Chen, J. F. Zhao and G. M. Li, *Renewable Sustainable Energy Rev.*, 2012, 2360–2364.
- 31 J. B. Wang, *PhD thesis*, Shanghai Jiao Tong University, 2017.
- 32 CHEARI, White Paper on WEEE Recycling Industry in China for 2019, *Home Appliance*, 2020, vol. 525, DOI: [10.3969/j.issn.1002-5626.2020.07.020](https://doi.org/10.3969/j.issn.1002-5626.2020.07.020).
- 33 Ministry of Ecology Environment of the PRC, *Soil and sediment-Determination of aqua regia extracts of 12 metal elements-Inductively coupled plasma mass spectrometry (HJ 803-2016)*, 2016.
- 34 I. N. Doyi, V. Strezov, C. F. Isley, T. Yazdanparast and M. P. Taylor, *Sci. Total Environ.*, 2020, **733**, 137931.
- 35 M. Heidari, T. Darijani and V. Alipour, *Chemosphere*, 2021, **273**, 129656.
- 36 S. N. Istanbulu, H. Sevik, K. Isinkaralar and O. Isinkaralar, *Bull. Environ. Contam. Toxicol.*, 2023, **110**, 78.
- 37 K. Loska, D. Wiechuła and J. Pelczar, *Commun. Soil Sci. Plant Anal.*, 2005, **36**, 1117–1128.
- 38 H. M. Li, J. H. Wang, Q. G. Wang, X. Qian, Y. Qian, M. Yang, F. Y. Li, H. Lu and C. Wang, *Atmos. Environ.*, 2015, **103**, 339–346.
- 39 F. S. Wei, G. Z. Yang, D. Z. Jiang, Z. H. Liu and B. M. Sun, *Environ. Monit. China*, 1991, **1**, 1–6.
- 40 J. H. Wang, S. W. Li, X. Y. Cui, H. M. Li, X. Qian, C. Wang and Y. X. Sun, *Ecotoxicol. Environ. Saf.*, 2016, **128**, 161–170.
- 41 L. Zhou, G. J. Liu, M. C. Shen, R. Y. Hu, M. Sun and Y. Liu, *Environ. Pollut.*, 2019, **251**, 839–849.
- 42 Y. Liu, T. Jin, S. H. Yu and H. Q. Chu, *Environ. Sci. Pollut. Res.*, 2023, 1–14.
- 43 C. M. Yesilkanat and Y. Kobya, *Geoderma Reg.*, 2021, **25**, e00388.
- 44 M. Gope, R. E. Mastro, J. George, R. R. Hoque and S. Balachandran, *Ecotoxicol. Environ. Saf.*, 2017, **138**, 231–241.
- 45 I. S. Shabanda, I. B. Koki, K. H. Low, S. M. Zain, S. M. Khor and N. K. Abu Bakar, *Environ. Sci. Pollut. Res.*, 2019, **26**, 37193–37211.
- 46 US EPA, *Exposure factors handbook*, 2011.
- 47 US EPA, *Risk assessment guidance for superfund volume I: human health evaluation manual (Part F, Supplemental guidance for inhalation risk assessment)*, Washington DC, 2009.
- 48 US EPA, *Supplemental guidance for developing soil screening levels for superfund sites*, United States Environ. Prot. Agency, 2002, vol. 12, pp. 1–187.
- 49 US EPA, *Appendix A: Water Pathway*, 2004.
- 50 US EPA, *Regional Screening Level (RSL) Summary Table*, 2012.
- 51 Ministry of Environmental Protection of the PRC, *Technical guidelines for risk assessment of contaminated sites (HJ 25.3-2014)*, 2014.
- 52 US EPA, *Emergency and R. Response, Risk Assessment Guidance for Superfund: pt. A. Human health evaluation manual*, Office of Emergency and Remedial Response, US Environmental Protection Agency, 1989.
- 53 S. Gupta and S. K. Gupta, *Environ. Geochem. Health*, 2022, 1–22.
- 54 R. B. O. Lead, *Office of Solid Waste and Emergency Response*, US Environmental Protection Agency, Washington, DC, 2007.
- 55 X. Hu, Y. Zhang, J. Luo, T. J. Wang, H. Z. Lian and Z. H. Ding, *Environ. Pollut.*, 2011, **159**, 1215–1221.
- 56 Y. H. Chai, M. X. Wang and X. Q. Zhao, *Environ. Chem.*, 2019, **38**, 1375–1384.
- 57 J. Zhang, L. Wu, Y. J. Zhang, F. H. Li, X. Z. Fang and H. J. Mao, *Particuology*, 2019, **44**, 146–152.
- 58 V. Kolakkandi, B. Sharma, A. Rana, S. Dey, P. Rawat and S. Sarkar, *Sci. Total Environ.*, 2020, **705**, 135805.
- 59 B. Schiavo, D. Meza-Figueroa, E. Vizuete-Jaramillo, A. Robles-Morua, A. Angulo-Molina, P. A. Reyes-Castro, C. Inguaggiato, B. Gonzalez-Grijalva and M. Pedroza-Montero, *Environ. Geochem. Health*, 2022, 1–22.
- 60 W. F. Liu, X. L. Hu, D. C. Zhang, L. Chen and T. Z. Yang, *Chin. J. Nonferrous Met.*, 2022, **32**, 2703–2713.
- 61 S. Ganesh, P. Danish and K. A. Bhat, *Mater. Today: Proc.*, 2021, **42**, 745–749.
- 62 X. X. Wei, C. C. Nie, Y. X. Yu, J. X. Wang, X. J. Lyu, P. Wu and X. N. Zhu, *Process Saf. Environ. Prot.*, 2021, **146**, 694–701.
- 63 L. Zhou, *PhD thesis*, University of Science and Technology of China, 2022.